Informing the SWAT model with remote sensing detected vegetation phenology for improved modeling of ecohydrological processes

Shouzhi Chen[1], Yongshuo H. Fu[1,2*],Zhaofei Wu[1], Fanghua Hao[1], Zengchao Hao[1], Yahui Guo[1], Xiaojun Geng[1], Xiaoyan Li[3], Xuan Zhang[1*], Jing Tang[4,5,6], Vijay P. Singh[7], Xuesong Zhang[8,9]

[1]College of Water Sciences, Beijing Normal University, Beijing 100875, China.

[2]Plants and Ecosystems, Department of Biology, University of Antwerp, Antwerp, Belgium.

[3]State Key Laboratory of Earth Surface Processes and Resource Ecology, Faculty of Geographical Science, Beijing Normal University, Beijing 100875, China

[4]Department of Physical Geography and Ecosystem Science, Lund University, Sölvegatan 12, SE-223 62, Lund, Sweden.

[5]Terrestrial Ecology Section, Department of Biology, University of Copenhagen, DK-2100, Copenhagen, Denmark.

[6]Center for Permafrost (CENPERM), University of Copenhagen, DK-1350, Copenhagen, Denmark.

[7]Department of Biological and Agricultural Engineering, Texas A&M University, College Station, Texas, USA.

[8]Joint Global Change Research Institute, Pacific Northwest National Lab, College Park, MD 20740, USA

[9]Great Lakes Bioenergy Research Center, Michigan State University, East Lansing, MI 48824, USA

Corresponding author: Yongshuo H. Fu () ; Xuan Zhang (Xuan@bnu.edu.cn)

Key Points:

- We improved the SWAT model with remote sensing-detected phenology and the improved model better simulated LAI.
- The original SWAT model significantly underestimated evapotranspiration compared with modified SWAT model.
- Growing season extended one day will induce evapotranspiration increase 11.1 mm across forests.

Abstract

The Soil and Water Assessment Tool (SWAT) model has been widely applied for simulating the water cycle and quantifying the influence of climate change and anthropogenic activities on hydrological processes. A major uncertainty of SWAT stems from poor representation of vegetation dynamics due to the use of a simplistic vegetation growth and development module. Using long-term remote sensing-based phenological data, we improved the SWAT model's vegetation

module by adding a dynamic growth start date and the dynamic heat requirement for vegetation growth rather than using constant values. We verified the new SWAT model in the Han River basin, China, and found its performance was much improved in comparison with that of the original SWAT model. Specifically, the accuracy of the leaf area index (LAI) simulation improved notably (coefficient of determination (R^2) increased by 0.193, Nash–Sutcliffe Efficiency (NSE) increased by 0.846, and percent bias decreased by 42.18%), and that of runoff simulation improved modestly (R^2 increased by 0.05 and NSE was similar). Additionally, we found that the original SWAT model substantially underestimated evapotranspiration (Penman–Monteith method) in comparison with the new SWAT model (65.09 mm (or 22.17%) for forests, 92.27 mm (or 32%) for orchards, and 96.16 mm (or 36.4 %) for farmland), primarily due to the inaccurate representation of LAI dynamics. Our results suggest that accurate representation of phenological dates in the vegetation growth module is important for improving the SWAT model performance in terms of estimating terrestrial water and energy balance.

Plain Language Summary

Aiming to reduce the uncertainty of SWAT performance, which is derived largely from poor simulation of vegetation dynamics attributable to the simplified vegetation module. We using long-term remote-sensing-based phenological data, and improved the SWAT vegetation module by adding a dynamic growth start date and the dynamic heat requirement for vegetation growth rather than using constant values. We validated the modified SWAT model through application to the Han River basin (China), and found that its performance was improved substantially in comparison with that of the original model. Specifically, the accuracy of the leaf area index (LAI) simulation was improved notably (coefficient of determination (R2) increased by 0.190, Nash–Sutcliffe Efficiency (NSE) increased by 0.840, and percent bias decreased by 42.05%), and that of runoff simulation improved modestly (R2 increased by 0.05 and NSE was similar). Additionally, we found that the original SWAT model substantially underestimated evapotranspiration (Penman–Monteith method) in comparison with the new SWAT model, primarily due to the inaccurate representation of LAI dynamics. Our results suggest that accurate representation of phenological dates in the vegetation growth module is important for improving the SWAT model performance in terms of estimating terrestrial water and energy balance.

1 Introduction

Vegetation, as the key factor connecting the soil and the atmosphere in a terrestrial ecosystem, plays a crucial role in the hydrological cycle [*Rodriguez-Iturbe*, 2000; *Sprenger et al.*, 2016]. Vegetation dynamics have many crucial effects on the terrestrial water cycle, such as rainfall interception, soil water transport, evapotranspiration, and soil property change [*Kergoat*, 1998; *Tesemma et al.*, 2015; *Webb and Kathuria*, 2012; *Wei and Zhang*, 2010; *D Zhang et al.*, 2018]. The Soil and Water Assessment Tool (SWAT) model considers vegetation dynamics using a simplified version of the Environmental Policy Impact Climate

(EPIC) growth module, which simulates the seasonal leaf area index (LAI) by employing a day length threshold and heat unit theory [*Arnold et al.*, 2012; *Williams et al.*, 1989]. Although previous studies [*Yang and Zhang*, 2016; *Yang et al.*, 2019] improved the SWAT model for simulating biomass accumulation of forests, it is not applicable to all regions because vegetation dormancy is affected by other complex environmental factors in addition to day length [*Rajib et al.*, 2020; *Strauch and Volk*, 2013; *Wagner et al.*, 2011]. Consequently, large uncertainties exist in the assessment of terrestrial water cycle conducted using such hydrological models [*H Zhang et al.*, 2020]. Therefore, it is essential to improve the vegetation simulation module used in hydrological models to improve our understanding of ecosystem hydrological response to ongoing climate change.

The growth dynamics of terrestrial vegetation are substantially influenced by ongoing climate change over recent decades [*Shukla et al.*, 2019]. For example, vegetated regions are exhibiting enhanced greening [*Piao et al.*, 2015; *Zhu et al.*, 2016], and phenology variation, such as spring advancement and autumn postponement, is occurring on the global scale [*Gill et al.*, 2015; *Jeong et al.*, 2011; *Piao et al.*, 2019]. One of the major shortcomings of the SWAT model, attributable to the use of the simplified EPIC module, is that the spatiotemporal heterogeneity of vegetation is ignored, which introduces challenges regarding the simulation of vegetation dynamics. By introducing either the soil moisture index or precipitation to track vegetation in the new growing season, the performance of SWAT model in the simulation of vegetation dynamics has been improved to a certain extent [*Strauch and Volk*, 2013; *Valencia et al.*, 2021]; however, such improvement is observed mainly in relation to evergreen forest vegetation in tropical areas (in SWAT defined as regions within latitudes between 20° S and 20° N), so widespread regional applicability is limited. The improved scheme of the Moderate Resolution Imaging Spectroradiometer (MODIS) LAI based on remote sensing observations has wide regional applicability, but it requires high-quality remote sensing data and increases the structural complexity of SWAT model simulations [*Ma et al.*, 2019; *Rajib et al.*, 2020]. The approach to defining vegetation growth dormancy using remote-sensing-based or observed vegetation phenology strikes a balance between model complexity and performance, making it a promising candidate to improve the performance of vegetation dynamics and hydrologic simulation by the SWAT model.

In this study, we use remote sensing-based Global Inventory Modeling and Mapping Studies 3rd generation ($GIMMS_{3g}$) normalized difference vegetation index (NDVI) data to extract dates of phenological events with five different methods, including threshold methods (e.g., Gaussian, Spline, and Savitzky–Golay) and change ratio methods (e.g., HANTS and Polyfit) [*Chen et al.*, 2004; *Cong et al.*, 2012; *Savitzky and Golay*, 1964]. We further link the phenological data with hydrological response units (HRUs) using area-weighted methods and modified the dormancy criteria of the vegetation module in the SWAT model. Specifically, the extracted phenological dates based on satellite data were used as input to determine vegetation dormancy in the HRUs, instead of simply using latitude and day length to determine vegetation dormancy. Meanwhile, on the basis

of remote-sensing-based phenological dates of each HRU, the accumulated heat unit required for vegetation growth in the current year is calculated, and the static accumulated heat unit constant in the vegetation database of the original SWAT model is replaced by the dynamic accumulated heat unit. To verify the applicability of the modified SWAT model, we tested the model for simulating LAI and runoff for the Han River basin, China.

This study aims to achieve three specific objectives: 1) obtain dates of vegetation phenology and its spatiotemporal patterns at the watershed scale, 2) improve the simulation accuracy and applicability of the SWAT model in terms of vegetation growth by improving the dormancy module through the addition of the dynamic accumulated heat unit module, and 3) explore the variation of vegetation-related hydrological parameters and their rationalities in the changed vegetation growth module.

2 Materials and methods

2.1 Study area

The Han River basin, China, is striding the boundary between the south of the temperate zone and the north of the subtropics (Fig. 1). It has a catchment area of 51,969 km^2 with elevation ranging from 266 - 3557 m. The mean annual temperature is 12.2 ℃, mean annual precipitation is 827.1 mm, and the mean annual runoff at the Ankang gauging station is 345.57 mm, averaged over the study period 2001 - 2014. Our study region is located in the upper Han River and includes a secondary tributary of the Yangtze River. Land use in the region changed little during 2001–2014, dominated by orchards (ORCD: 37% of the area), forests (FRST: 36%), and farmland (AGRL: 26%) (Fig. 1c). Since the 1990s, areas of ORCD and FRST that are distributed evenly throughout all sub-basins and accounted for >70% of the total area; conversely, AGRL areas tend to be distributed mainly in several sub-basins in the upstream of the basin.

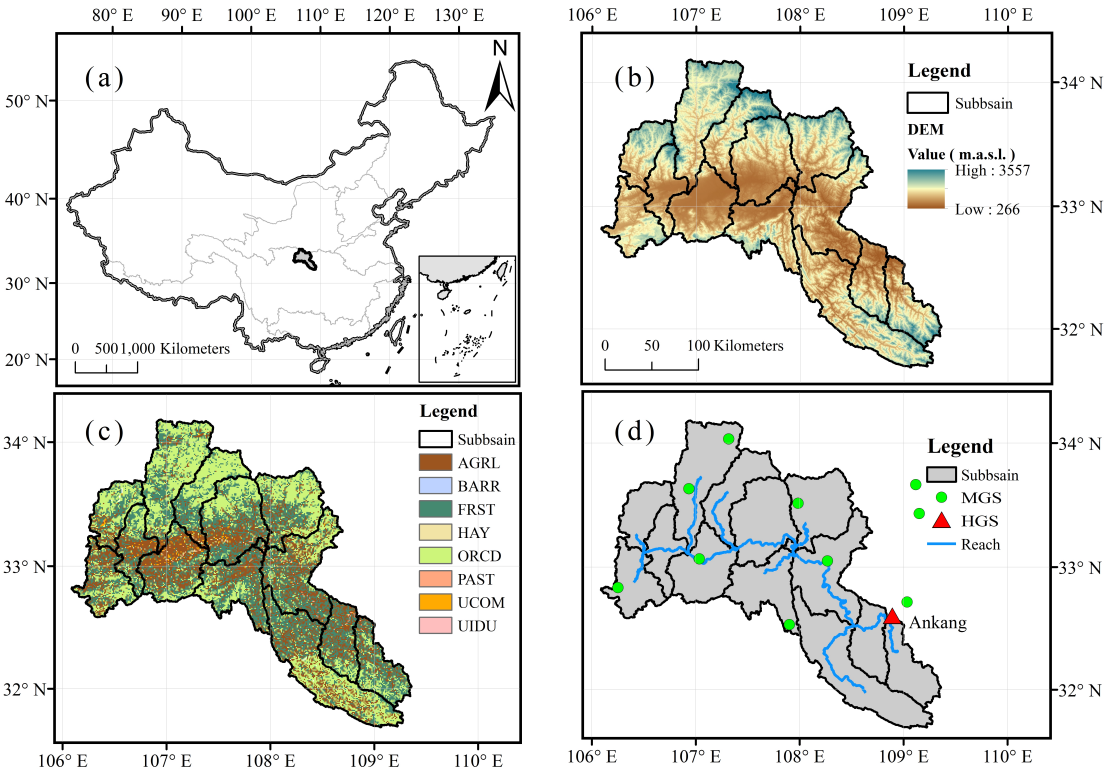

Figure 1. (a) Location of the Han River basin, (b) its elevation, (c) distribution of its land use types, and (d) locations of the meteorological observation stations (MGSs) and hydrological gauging station (HGS). Notably, AGRL (farmland), FRST (forests), and ORCD (orchards) land use types represent the major vegetation types used to mask the Global Land Surface Satellite leaf area index dataset. BARR - bare land, HAY - hay land, PAST - pasture, UCOM - commercial land, and UIUD - industrial land.

2.2 Input datasets

2.2.1 Digital elevation model (DEM), land use, and soil data The data used in this study and their sources are presented in Table 1. In the ArcSWAT toolbox, a 90-m spatial resolution digital elevation model (DEM) [Jarvis et al., 2008] was used to delineate the watershed and river network and generate 14 sub-basins (Fig. 1d). SWAT primarily relies upon defined HRUs that are based on land use maps, soil maps, and slope characteristics. In this study, 384 HRUs were defined using a multiple HRU generation method incorporating land use, soil, and slope inputs (thresholds of 10%–10%–10%) using the SWAT2012 extension (version 1.9) within ArcGIS 10.2 software (Environmental Systems Research Institute, Inc).

The land use data were developed by the Center for Resources and Environmental Sciences and Data, Institute of Geographic Sciences and Natural Resources Research, Chinese Academy of Sciences (https://www.resdc.cn/). Data production was based on Landsat TM/ETM remote sensing images of each period generated through manual visual interpretation. This dataset with 1-km spatial resolution was used and reclassified to match the SWAT land use classes adopted for HRU delineation in the SWAT model (Fig. 1a). Eight SWAT land use types were identified in this river basin in 2005 (Fig. 1c): AGRL, FRST, ORCD, BARR (bare land), HAY (hay land), PAST (pasture), UCOM (commercial land), and UIUD (industrial land).

The Harmonized World Soil Database is a 30-arcsecond raster database with over 15,000 different soil mapping units that combines existing regional and national updates of soil information worldwide (SOTER, ESD, Soil Map of China, WISE) with information contained within the 1:5,000,000 scale FAO-UNESCO Soil Map of the World (FAO, 1971–1981) [Nachtergaele et al., 2010]. We clipped these datasets for SWAT model generation in the Han River basin using watershed polygons delineated previously in ArcGIS 10.2.

2.2.2 Observed meteorological, runoff, and leaf area index data It can be seen from Table 1 that daily in situ measurements of observations (precipitation, maximum and minimum daily temperatures, rainfall, relative humidity, wind, and solar radiation) were obtained from the National Meteorological Information Center (http://data.cma.cn/). Daily runoff data (2001–2014) from the Ankang hydrological station, which is located at the catchment outlet, were obtained from the Hydrological Bureau of the Ministry of Water Resources of China. The LAI data were taken from the Global Land Surface Satellite (GLASS) product (spatial resolution: 0.05°, temporal interval: 8 d), produced using Advanced Very High Resolution Radiometer time series surface reflectance data acquired during 1981–1999. Since 2000, the GLASS product has been generated using MODO9A1 surface reflectance data in sinusoidal projection at the global scale from Advanced Very High Resolution Radiometer and Moderate Resolution Imaging Spectroradiometer reflectance data using a general regression neural network [Xiao et al., 2013]. The GLASS LAI product (version 3.0) is freely available for download from http://glass-product.bnu.edu.cn. The GIMMS3g NDVI dataset, obtained from the Ecological Forecasting Lab (https://ecocast.arc.nasa.gov/data/pub/gimms/), encompassed the period from July 1981 to December 2015 (spatial resolution: 1/12°, temporal resolution: 15 d).

Table 1. Details of the data used in this study.

Data	Source	Description
DEM	CGIAR CSI	SRTM Derived DEM (90 m)

Data	Source	Description
Land use/Land cover map	Resource and Environment Science and Data Center	km spatial resolution
Soil map	FAO[1]	Harmonized World Soil Database v 1.2
Observed Meteorological data	National Meteorological Information Center	Maximum and minimum daily temperature, rainfall, relative humidity, wind, solar radiation (2001-2014)
Observed runoff	the Hydrological Bureau of the Ministry of Water Resources of China (HBMWRC)	Ankang (daily, 2004-2014)
Leaf area index	GLASS	day / 0.05°×0.05°
Normalized difference vegetation index	$GIMMS_{3g}$	day / 0.05°×0.05°

[1]FAO: Food and Agriculture Organization.

2.3 Overview of the SWAT model

The SWAT model, developed by the U.S. Department of Agriculture's Agricultural Research Service, is a semi-distributed hydrological model based on physical processes [Arnold et al., 1998; Neitsch et al., 2011]. It can simulate different fluxes within the hydrological cycle, such as evapotranspiration (ET), surface runoff, percolation, lateral flow, groundwater flow, transmission, and ponding over long periods. In the SWAT model, an entire river basin is divided into many HRUs based on slope, soil type, and land use type. The model simulates the spatial variation of the river basin on the basis of hydrological dynamics of each HRU, and then performs water routing for the river channel [Arnold et al., 2012]. Current research on improving the vegetation growth module of the SWAT model is mainly based on defining dry and wet seasons through the soil moisture index or precipitation, thereby tracking the beginning of new vegetation growing season and better simulating vegetation growth dynamics [Alemayehu et al., 2017; Ma et al., 2019; Rajib et al., 2020; Strauch and Volk, 2013; Valencia et al., 2021].

Vegetation dynamics play an important part in the hydrological cycle. The SWAT model simulates annual LAI dynamics of different vegetation types (warm season annual legumes, cold season annual legumes, perennial legumes, warm season annuals, cold season annuals, perennials, and trees) in each HRU to reflect the vegetation dynamics within the river basin to a certain extent.

The vegetation module of the SWAT model is a simplified version of the EPIC model, which simulates vegetation growth mainly on the basis of two theories: heat unit theory and day length threshold theory [Williams et al., 1989].

2.3.1 Plant growth module in SWAT Temperature is one of the most important of the various factors that control plant growth. Each plant has a temperature range suitable for growth, i.e., the lowest, most suitable, and highest temperatures at which plant growth can occur. For each plant, the minimum or base temperature must be reached before the plant will begin to grow. Generally, above the base temperature, the higher the temperature, the faster the growth rate [*Jobling*, 1997]. However, once the optimum temperature for plant growth is exceeded, the rate of growth begins to slow, and when the maximum temperature is reached, growth stops. The heat unit theory assumes that the plant growth trajectory (such as plant maturation) is proportional to the temperature increment. When the average temperature is lower than the base temperature, the plant will no longer grow, and when the daily average temperature exceeds the base temperature, the plant will grow [*Boswell*, 1926; *Magoon and Culpepper*, 1932]. Heat units in the SWAT model are calculated using a direct summation index, with one heat unit for each degree Celsius of daily mean temperature above the base temperature. However, application of the heat unit theory in the SWAT model does not consider the influence of harmful high temperatures on plants; instead, it is assumed that all temperatures higher than the base temperature will accelerate the growth and development of crops.

The heat accumulation unit for a given day is calculated as follows:

$$\overline{\qquad}, \quad (1)$$

where is the heat unit accumulated on a given day, is the average daily temperature (℃), and represents the base or minimum temperature required for plant growth (℃).

The total heat units required for a plant to reach maturity is calculated as follows:

$$\overline{\qquad}, \quad (2)$$

where denotes the total heat units required for a plant to reach maturity, is the accumulated heat unit on day d, where d = 1 represents the sowing date or the end date of the dormant period, and m is the number of days needed for the plant to reach maturity. It should be noted that could also represent potential heat units.

In the SWAT model, the dormant date is defined by day length threshold theory.

When the day length reaches the calculated threshold for a given location, plant dormancy will occur. The day length threshold is calculated as follows:

$$\overline{\quad}, \quad (3)$$

where is the threshold of day length at the beginning of the dormant period (h). is the shortest day length in a year in the river basin (h), and is the hibernation threshold (h). In autumn, when day length is shorter, plants in the catchment, except warm-season annuals, enter a dormant period. The dormant threshold varies with latitude as follows:

$$\overline{\quad}, \quad (4)$$

$$, \quad (5)$$

$$, \quad (6)$$

where denotes the dormancy threshold, which is used to reflect the difference of dormancy time at different latitudes (h), and denotes the latitude in positive values (°).

There are theoretical uncertainties in the two theories mentioned above when simulating the growth process of vegetation. First, the dormant period of vegetation is judged simply on the basis of latitude and photoperiod, whereas complex interactions between different environmental factors actually determine the dormancy period and the starting conditions [Rohde and Bhalerao, 2007]. The current approach in SWAT ignores the differences in dormancy period of vegetation at different locations at the same latitude. Second, the accumulated heat unit demand of each plant of a particular land use/land cover (LULC) is given as a constant value, which is inconsistent with the findings of previous studies showing that heat requirements change with growing conditions. For instance, a warmer winter can enhance the accumulated heat unit requirements of plants by reducing the chilling period of vegetation [Wang et al., 2020; Yu et al., 2010]. The accumulated heat units required by vegetation change annually, and the use of a fixed accumulated heat unit requirement can lead to large uncertainties in the length of the simulated growing season.

2.3.2 Development of the growth module in SWAT Recognizing the aforementioned limitations, vegetation growth cycles should be initiated dynamically rather than through management operations (e.g., "plant" and "kill") that prescribe the dates or fractions of PHU for each simulation year. Thus, we modified the vegetation dormancy and accumulated heat unit requirement of the original SWAT2012 model Version. 681 (https://swat.tamu.edu), so that no management operation was applied during the set-up of the modified model. In the following sections, we explain the specific principles and details of model

improvements (Fig. S1).

2.3.2.1 Phenology extraction The dates of occurrence of phenological events are critical in the vegetation growing season. In this research, five different phenological extraction methods (i.e., the HANTS-Maximum method, Spline-Midpoint method, Gaussian-Midpoint method, Timesat-SG method, and Polyfit-Maximum method) [Cong et al., 2012; Savitzky and Golay, 1964] were used to estimate spring (start of growing season; SOS) and autumn (end of growing season; EOS) phenological events in the Han River basin using the GIMMS3g NDVI data. Two processes were applied to extract the phenology data: 1) application of smoothing and interpolation to obtain daily time series NDVI data, and 2) use of the phenological phase extraction method based either on the threshold value (here, we used 0.5 and 0.2 as the threshold for SOS and EOS, respectively) or the maximum rate of change [*Piao et al.*, 2006; *Reed et al.*, 1994; *White et al.*, 1997; *White et al.*, 2009]. To reduce uncertainties associated with a single method, the mean value of the extracted phenological indexes from the five methods was used as the phenology data for the studied river basin.

2.3.2.2 mapping grid phenology value into HRUs The phenological events derived from remote sensing NDVI data have a spatial resolution of 0.05°, whereas the simulation of the hydrological cycle process in the SWAT model is based on HRUs. Providing annual phenological records to each HRU by linking the phenological data with each HRU is the premise for further model improvement. We leveraged the technology of the SWAT-Modflow method [Kim et al., 2008] to build a fishnet in ArcGIS 10.2 software to match the gridded data with the spatial position of each HRU, and generate statistics for the grid cells by averaging the gridded values over each HRU (Fig. 2).

The average phenological dates (i.e., SOS and EOS) for the each HRU were estimated on the basis of weighted coefficients calculated from the area size of the overlapped region to reconcile the spatial mismatch between the grid phenology data and the irregular polygons of the HRUs used in the SWAT model simulation. The area weight of the HRU phenological period was determined as follows:

$$\text{, } \quad (7)$$

where stands for the phenology date (i.e., SOS or EOS) of a year for a given HRU, denotes the total area of a given HRU, represents the phenology data value of the grid in which the i-th subblock of the HRU is located, represents the area occupied by the i-th subgrid, and n is the number of overlapping subblocks into which the HRU is divided.

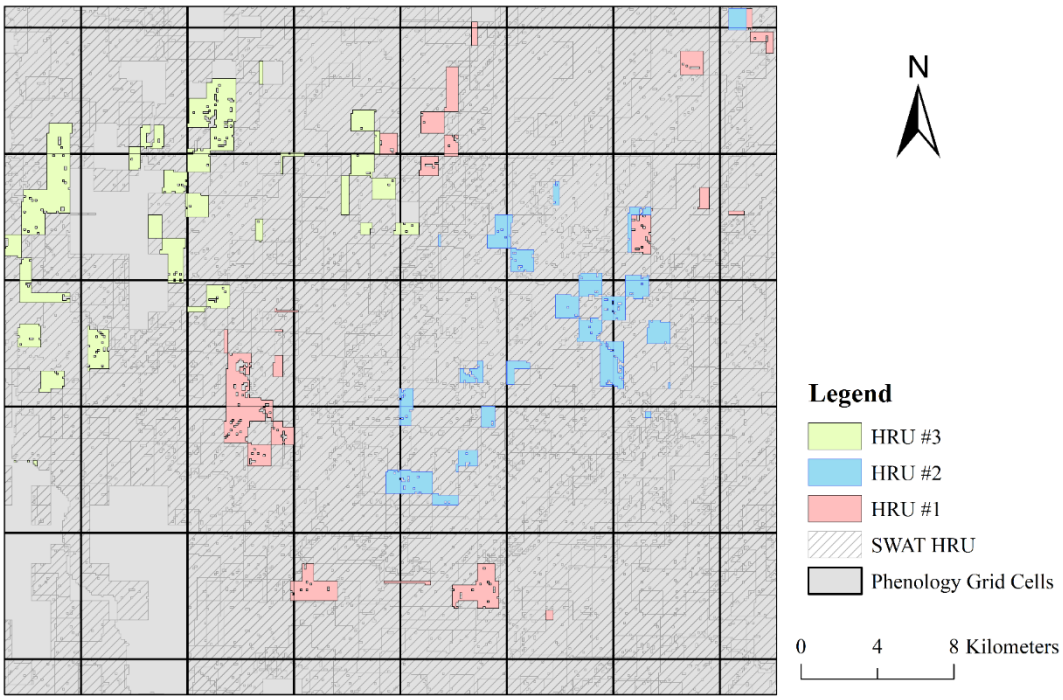

Figure 2. Overlapped areas of hydrological response units (HRUs) and gridded phenology data. Dark gray grid represents the gridded phenology data, light gray background represents the SWAT HRUs of the Han River basin, and selected HRUs #1–3 show different cases of how HRUs intersect with phenology grid cells.

2.3.2.3 Dormant module modification In this study, we modified the source code of the plant dormancy module of the SWAT model (dormant.f) used for determining the dormant status of vegetation. For trees with a vegetation type index of 7 (e.g., FRST and ORCD), the day length threshold is no longer used to determine whether the trees are at the critical point between the dormancy period and the growing season. Instead, the extracted phenology data were used to determine the growth state of trees on a simulated day, and the accuracy of the model simulation was optimized on the basis of the actual growth state of trees. We also modified the LAI modeling during leaf senescence for perennials using the approach introduced by Strauch and Volk (2013) (Fig. 3):

, (8)

, (8)

, (9)

where the term used as the exponent is a function of time () and ranges from 6 to −6; is the leaf area index for a given day that declines at rate r; and are the maximum and minimum (ALAI_MIN, minimum LAI for the plant during the dormant period (m^2/m^2)) LAI values, respectively; and is the fraction of the growing season () over which senescence becomes the dominant growth process.

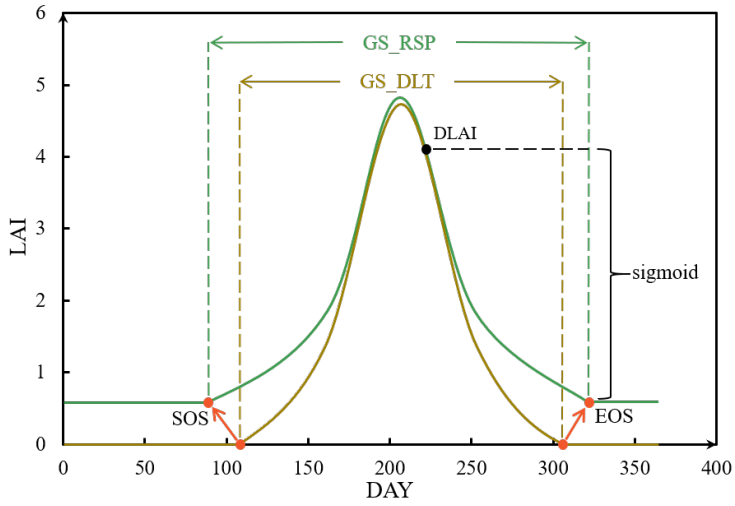

Figure 3. Principles of the developed vegetation dormancy module in the Soil and Water Assessment Tool model. SOS - start of growing season, EOS - end of growing season, GS_DLT - growing season defined by day length threshold, GS_RSP - growing season defined by remote sensing phenology. Orange dots indicate occurrence dates of phenology events, and black dot indicates DLAI, i.e., the fraction of the total heat units when leaf area begins to decline. Sigmoid: a logistic decline curve shown in the study by Strauch and Volk (2013).

2.3.2.4 Dynamic heat unit requirement In the modified SWAT model, we calculated the accumulated heat unit requirement (i.e., the average daily temperature above base temperature BASE_T between SOS and EOS) for annual vegetation growth using the remote sensing vegetation phenology. The calculated value (PHU_PLT) was used to replace the fixed accumulated heat unit requirement for specific plants in the plant parameters database (plant.dat) (Fig. 4).

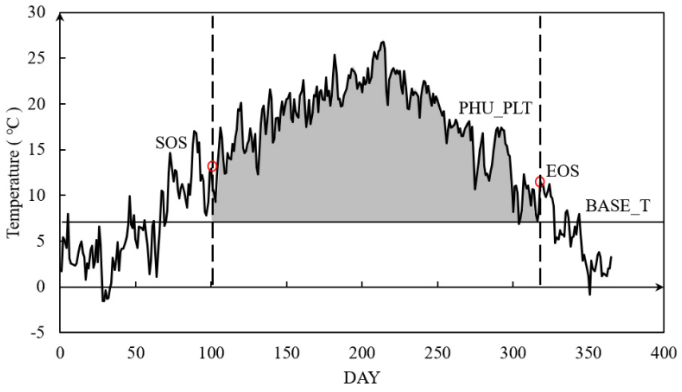

Figure 4. Dynamic heat unit of vegetation growth module in the Soil and Water Assessment Tool model. The gray areas represent the accumulated heat unit requirement for plant growth in a given year. SOS - start of growing season, EOS - end of growing season, BASE_T - minimum temperature for vegetation growth, PHU_PLT - heat unit requirement of vegetation in the current year.

2.3.2.5 Model calibration and validation In this study, the stepwise calibration method was adopted for the modeled LAI and runoff in the modified model. Calibration of runoff and LAI was conducted for 2004–2010 and validation was performed for 2011–2014. For the original model we only calibrated runoff, but the time series used for calibration and validation were the same as those used for the modified model. To obtain comparable results, and for the assessment of the effect of inaccurate representation of vegetation dynamics, the original SWAT model was not calibrated for LAI, which is not an unusual practice [Alemayehu et al., 2017; Rajib et al., 2020; Valencia et al., 2021; Villamizar et al., 2019]. Three years were added at the beginning of each simulation as a spin-up period necessary to approximate initial conditions, especially for soil moisture.

We used ENVI 5.3 software to clip the GLASS LAI with three main LULC types (FRST, ORCD, and AGRL) using the HRUs as borders, and all raster data belonging to the same LULC type were extracted and their average values taken as the observed LAI values in the study area. Calibration of LAI through a combination of manual (trial-and-error process) and automatic (particle swarm optimization) [Marini and Walczak, 2015] methods was performed to determine the optimum parameters in the plant database (plant.dat). For the initialization of parameters, we restricted the parameters to be generated within truly acceptable intervals (e.g., ALAI_MIN, BALI, DLAI FRGRW1, FRGRW2, LAIMX1, LAIMX2, and T_BASE). It should be noted that PHU_PLT, the total number of heat units or growing degree days needed to bring plants to maturity, does not need to be calibrated because it is a dynamic value determined by the

accumulated heat unit module. To evaluate the agreement between the simulated and observed LAI values, we used the coefficient of determination (R^2), which describes the proportion of the variance in measured data explained by the model, percent bias (PBIAS), and Nash–Sutcliffe Efficiency (NSE).

The second step of the stepwise calibration method was runoff calibration. We calibrated both the modified and the original SWAT model. In SWAT-CUP 2019 (Version 5.2.1) [Abbaspour, 2008; Arnold et al., 2012], we used the Sequential Uncertainty Fitting (Sufi-2) algorithm to conduct sensitivity analysis, uncertainty analysis, and automatic parameter calibration process [Abbaspour et al., 2004]. For sensitivity analysis, following the literature, we selected 26 parameters that have greatest impact on the hydrological process, and then 12 of the most sensitive parameters were yielded for model calibration. The value range of each of these parameters was defined within an acceptable true and reliable range. The Sufi-2 algorithm was used to calibrate model parameters for daily runoff data. In each iteration we applied 1000 simulations and updated the parameter ranges with the next iteration selection via Latin hypercube sampling [Stein, 1987]. To compare the differences in runoff simulation performance between the original SWAT model and the modified SWAT model, we adopted the performance criteria proposed by Moriasi (2013)that included NSE, R^2, and PBIAS (bad: <0.5; not good: 0.5~0.65 ; good: 0.65~0.75; very good: >0.75) [Moriasi et al., 2007].

3 Results

3.1 Phenology in the Han River basin

There is clear spatial heterogeneity in vegetation phenology in the Han River basin (Fig. 5). For the entire basin, the SOS ranged from day of year (DOY) 81–118 (average: DOY 104), i.e., a difference of 37 d. The EOS ranged from DOY 280–341 (average: DOY 325), i.e., a difference of 61 d. The spatial distribution pattern was similar to that of LULC type (Fig. 1c). The SOS was the earliest for AGRL, followed by FRST and then ORCD. Similarly, the EOS was the earliest for AGRL, followed by FRST and then ORCD, although there was no significant difference in EOS between FRST and ORCD. The SOS of the entire Han River basin had experienced significant advance (−0.52 d/year) during 1982–2015, whereas the EOS had not shown an obvious trend of change (−0.02 d/year). Significant EOS delays were found in small parts of the upper and lower reaches of the Han River basin, while significant EOS advances were found in the middle reaches. At the same latitude, there were evident differences in vegetation phenology, and in the same region (grid), phenology can change markedly over time. This contrasts the assumptions made in the EPIC model regarding the dominant role of latitude in plant dormancy [Arnold et al., 2012; Williams et al., 1989].

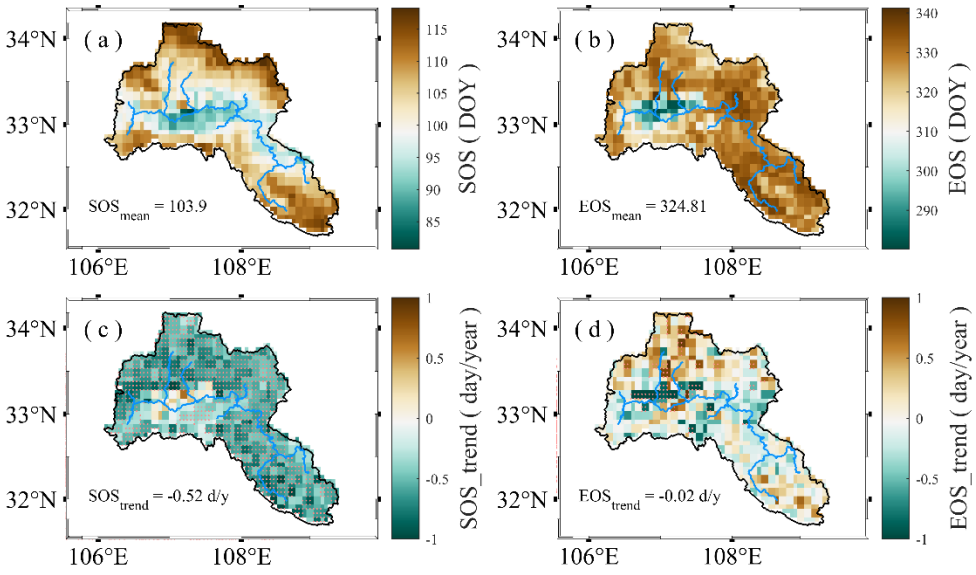

Figure 5. Spatial pattern and change trend of annual dates of occurrence of phenology events in the Han River basin during 1982–2015. SOS - start of growing season, EOS - end of growing season, DOY - day of year. Solid black line represents river basin boundary, and solid blue line represents the main river channel. Yellow dots indicate areas of significant change.

3.2 LAI calibration and validation

The optimum calibrated parameters in the SWAT plant database (plant.dat) are listed in Supplementary Table S1. The performance of the original SWAT model in simulating LAI was worse than that of the modified SWAT model, and the original SWAT model failed to represent the observed LAI curve and extreme values, as evidenced by the high biases and negative or low correlations (Table 2). Moreover, the original SWAT model could not match the remote sensing data in terms of either the value or the key time nodes of the LAI curve of the vegetation growth period. There are two principal shortcomings in the performance of the original SWAT model (Fig. 6): 1) inaccuracy in the LAI extreme value simulation, and 2) inaccuracy in the simulation of both the growing season length and the time nodes of the dormant period. With regard to the first, the simulated highest and lowest LAI values were different from the measured LAI determined by remote sensing. The SWAT model assumes that LAI is zero at the beginning of each simulation year, which is unrealistic for vegetation dynamics. With regard to the second, the growing season of the

simulated LAI curve of the original SWAT model did not correspond well to the growing season of the remote sensing LAI curve, there was mismatch between the start and end dates of the growing season, and the length of the growing season was not in accord with the actual situation. In contrast, the simulation performance of the modified SWAT model in relation to FRST and ORCD was better than that for AGRL. Overall, the modified SWAT model outperformed the original SWAT model in reproducing LAI observations and intra-annual LAI variations, as indicated by the correlation values.

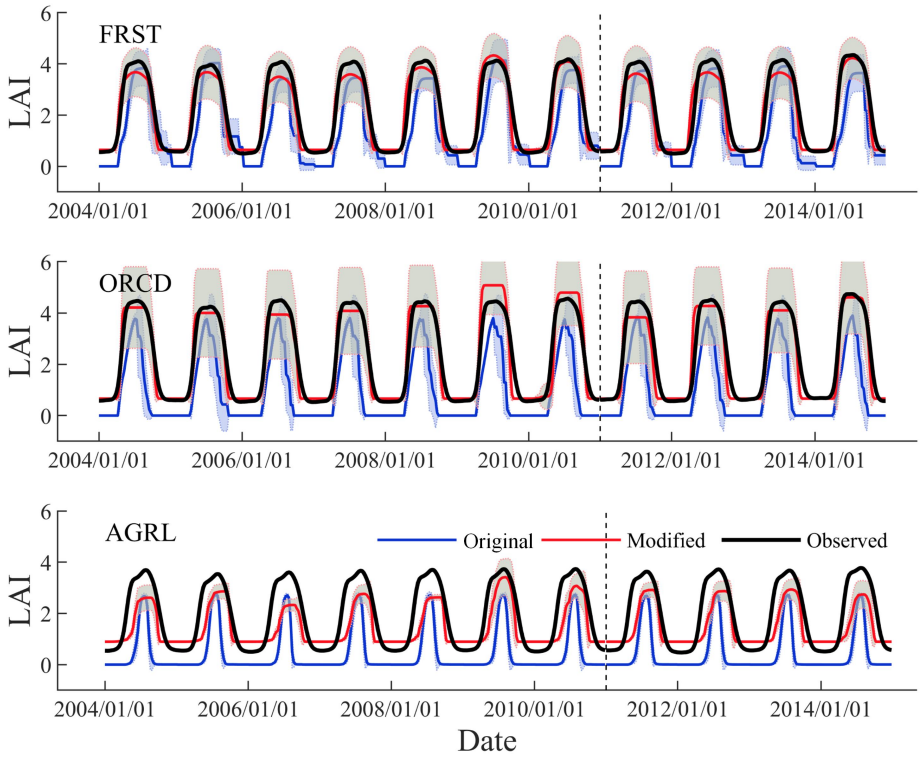

Figure 6. Global and Land Surface Satellite leaf area index (LAI), and the original and modified Soil and Water Assessment Tool model simulated hydrological response unit weighted aggregated 8-d LAI time series (2004–2014). Gray shading indicates the boundaries of the standard deviation. Dashed lines mark the end of the calibration period and the beginning of the validation period.

Table 2. Summary of the performance metrics for the original and modified Soil and Water Assessment Tool model in simulating leaf area index.

Performance criteria	Original (2004-2010)	Modified (2004-2010)	Original (2011-2014)	Modified (2011-
	FRST	ORCD	AGRL	FRST
R^2	0.83	0.75	0.49	0.95
NSE	0.69	0.12	-0.86	0.95
PBIAS	22.1	57.2	75.94	5.83

R^2, coefficient of determination, NSE, Nash–Sutcliffe Efficiency, PBIAS, percent bias, FRST, forests, ORCD, orchards, AGRL, farmland.

3.3 Runoff calibration and validation

The original and modified SWAT models were both calibrated for runoff by varying 12 of the most sensitive runoff-related parameters determined by sensitivity analysis (Supplementary Table S2). We found that the sensitivity of runoff to these parameters changed to differing degrees after the modification of the SWAT model, which meant that the order of the 12 most sensitive parameters was not the same for the two models. The best-fit parameters of two SWAT models and their acceptably ranges (i.e., the ranges of parameter values in each simulation that were acceptable for reality) after calibration are listed in Supplementary Table S3. Comparison of daily original SWAT model and modified SWAT model simulated runoff and multiple criteria evaluation results with observations for the calibration (2004–2010) and validation (2011–2014) periods are presented in Fig. 7. Visually, the simulated hydrographs presented a reasonable reproduction of observations. The R^2, NSE, and PBIAS (multiple criteria) results showed that both the original and the modified SWAT models could be considered "good" (0.65 NSE 0.75, 0.65 R^2 0.75), and the runoff simulation of both SWAT models showed better performance in the validation period than in the calibration period. The modified SWAT model was superior to the original SWAT model in terms of runoff simulation, as evidenced by the higher R^2 and NSE values in the calibration and similar in the validation periods. Nevertheless, the original SWAT model can show high performance in reproducing runoff by applying different parameter values with the same effect, despite having low capability in simulating LAI dynamics (Figs. 6 and 7).

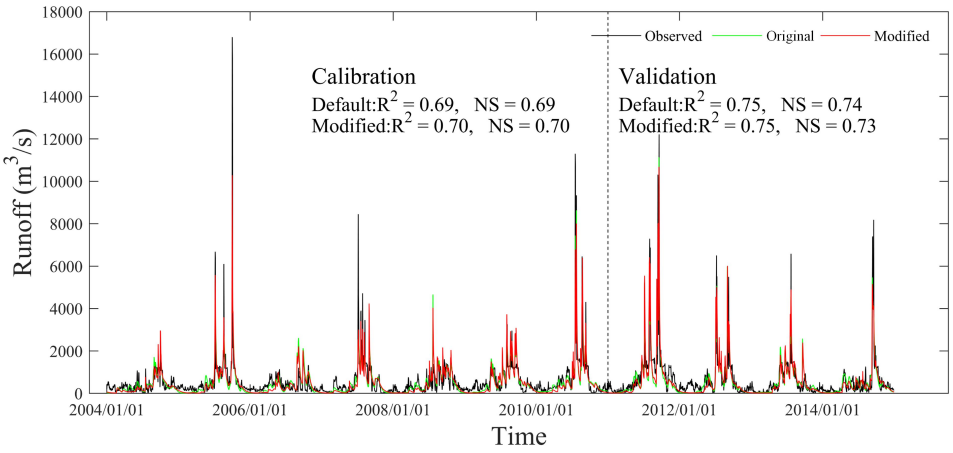

Figure 7. Calibration (2004–2010) and validation (2011–2014) of the original and modified Soil and Water Assessment Tool models for daily runoff. R^2 - coefficient of determination, NSE - Nash–Sutcliffe Efficiency. Dashed line marks the end of the calibration period and the beginning of the validation period.

3.4 Impact of improved LAI simulation on evapotranspiration

In basin-scale hydrological simulation, vegetation dynamics mainly regulate the hydrological cycle process by influencing ET. There are three main methods for SWAT to simulate ET: the Penman–Monteith method [Allen, 1986; Allen et al., 1989; Monteith, 1965], Priestley–Taylor method [Priestley and TAYLOR, 1972], and Hargreaves method [Hargreaves and Samani, 1985]. The Penman–Monteith method is a popular method that has been used in many previous studies [Abiodun et al., 2018; Parajuli et al., 2018]. The Penman–Monteith method includes the energy required to maintain evaporation, length of path of water vapor transport, aerodynamic factors, and surface impedance factors. Primarily, vegetation influences ET by influencing aerodynamic impedance and vegetation canopy impedance parameters. Theoretically, a more accurate simulation of vegetation dynamics and a more realistic LAI should bring more accurate performance in ET simulation. The difference in the ET simulation results between the modified SWAT model and the original SWAT model is believed caused by the difference attributable to dynamic simulation of vegetation growth. We found that the simulated ET value of the modified SWAT model was higher (65.09 mm (22.17%) for FRST, 92.27 mm (32%) for ORCD, and 96.16 mm (36.4 %) for AGRL) than that of the original SWAT model, and that this difference occurred mainly in spring and autumn. (Figs. 8 and S2). Moreover, there was significant underestimation of ET in the original SWAT model simulation compared with the modified SWAT model, especially in spring and autumn.

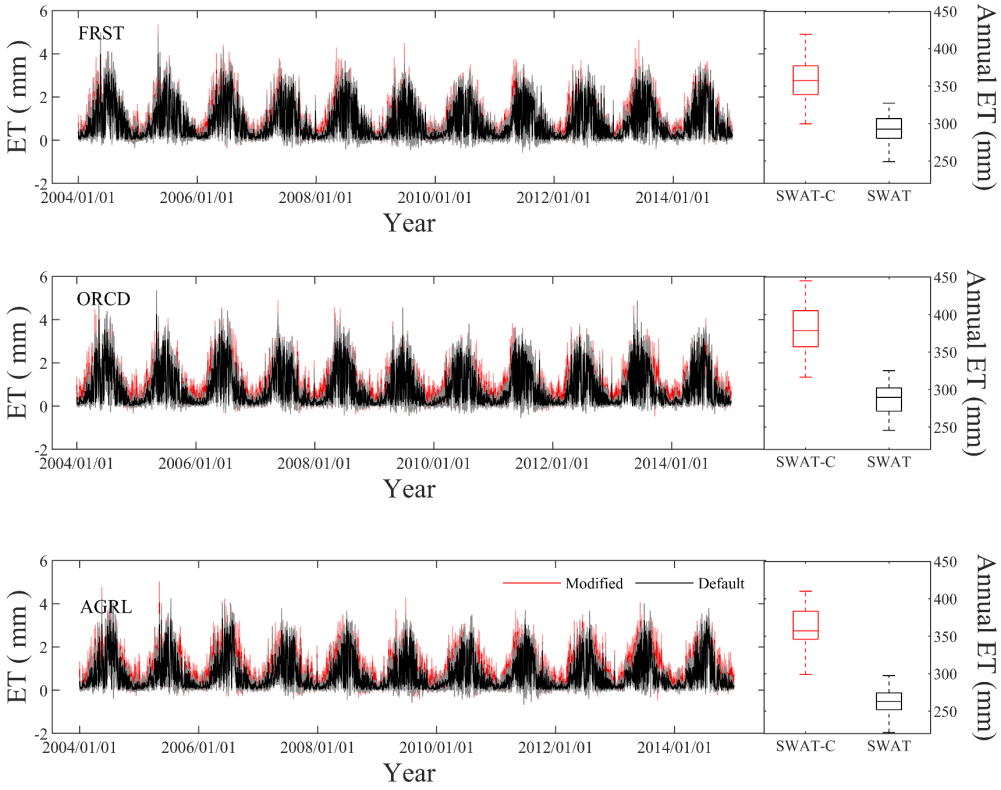

Figure 8. Daily evapotranspiration (ET) simulation during calibration (2004–2010) and validation (2011–2014) periods of the original and modified Soil and Water Assessment Tool models and corresponding annual ET box plots. Black crosses represent outliers.

4 Discussion

4.1 Changes of phenology on the basin scale

In this study, the temporal and spatial distribution characteristics of phenology in the Han River basin were extracted (Fig. 5), and the results revealed that phenology had a multiyear change trend and spatial dissimilation that was universal in different regions of the Northern Hemisphere [Badeck et al., 2004; Peñuelas and Filella, 2009; Piao et al., 2019]. Phenology shows different patterns with consistent but differing degrees of trend (i.e., SOS advance and EOS delay) in different climatic zones, and their responses to climate change were different owing to complex interactions among various environmental factors (e.g., temperature, photoperiod, precipitation, and radiation) [Delbart et al., 2008; Y

H Fu et al., 2015; Andrew D Richardson et al., 2006; Andrew D. Richardson et al., 2013; Yuan et al., 2020].

The phenological distribution and variation characteristics of vegetation were closely related to climatic zone and vegetation type. In the simulation of vegetation growth dynamics on the basin scale, a single and simple method that cannot accurately track the spatial and temporal variation of characteristics of vegetation phenology would increase the simulation error and uncertainty. Thus, the simulation of the entire hydrological energy cycle could be influenced by the effect on ET and other processes.

4.2 Advantages of the modified SWAT over the original SWAT model

There are notable differences between the modified and original SWAT models in terms of their capability in reproducing vegetation dynamics through LAI (Fig. 6). For example, the simulation performance of the modified SWAT model for both FRST and ORCD was better than that for AGRL, which was primarily because only the dynamic accumulated heat unit was considered in AGRL and no management operation was set in this study. In fact, irrigation and other management operations existed in AGRL. Moreover, the modified SWAT model also improved the simulation accuracy of runoff to some extent (Fig. 7). Although the modified and original SWAT models both achieved "good" runoff simulation performance, two different sets of model parameters were obtained in the process of runoff calibration. This is because one of the shortcomings of reverse modeling is that there could be cases where different sets of parameters in the model produce the same effect [Beven, 2002; Ruddell et al., 2019]. The relationship between annual ET and growing season length simulated by the original and modified SWAT models revealed that the original SWAT model not only had considerable uncertainty in terms of the simulation of growing season length, but also the relationship between ET and growing season length in the simulation results was inconsistent with that of previous studies [Geng et al., 2020], while the modified SWAT model revealed that growing season extended one day will increase evapotranspiration by 11.1 mm across forests. The improved model resolved these two problems (Fig. 9) that strongly limit the capability of hydrological models (i.e., the original SWAT model in the present case) to produce reliable results that could support informed decision-making [Kirchner, 2006; Valencia et al., 2021].

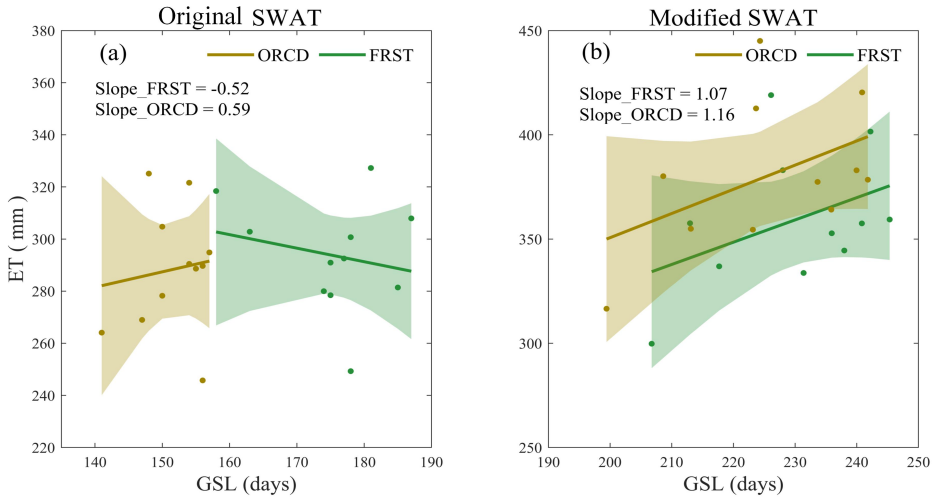

Figure 9. Relationship between the average annual evapotranspiration (ET) simulation performance of the modified and original Soil and Water Assessment Tool models and growing season length. FRST - forests, ORCD - orchards, GSL - growing season length. Shaded areas represent 95% confidence intervals.

The dormant period of vegetation was determined using vegetation phenology extracted from remote sensing rather than by indirectly tracking key nodes of vegetation growth using environmental factors (e.g., precipitation and soil moisture index) [Alemayehu et al., 2017; Strauch and Volk, 2013; Valencia et al., 2021]. It means that there was no need to consider differences in plant sensitivity to environmental factors in different regions, which can lead to more accurate simulation of vegetation growth dynamics in a wider region.

Although coupling the remote sensing-based phenology datasets substantially improved the SWAT performance, two limitations of the present study need to be pointed out. First, the simplified EPIC model based on accumulated heat unit was still used in this study to simulate vegetation growth dynamics, whereas more complete vegetation growth model should be used in subsequent studies. Second, in this research, the SWAT model was modified by integrating observed phenology data, but we could not predict the hydrological processes under future climate change. Here we explored the importance of phenology for hydrology process based models, and note that the next step is to further improve the model prediction of phenological events under future climate change conditions. The hydrological processes can be investigated by combining the phenology data which was simulated by phenological model under future climate change context. However, the accuracy of the current phenological model still needs to be improved [Y Fu et al., 2020; Liu et al., 2016; Andrew D Richardson et al., 2012], therefore we caution that in the subsequent studies, we need to improve the accuracy of phenological model and couple it with hydrological

models to ensure an accurate simulation of ecohydrology process under future climate change conditions [Chuine and Régnière, 2017; Fan et al., 2020; Hufkens et al., 2018].

5 Conclusions

In this study, the vegetation growth module of the SWAT model was improved using remote sensing-based vegetation phenology by optimizing the determination plant dormancy and the use of dynamic accumulated heat unit requirement by plants. We compared the modified SWAT model with the original SWAT model in the Han River basin. The results show that the modified model greatly improved the simulation of vegetation growth dynamics, and slightly improved runoff simulation. We also found that the original SWAT model significantly underestimated ET in different LULC types as compared with the modified SWAT model. Analysis of the relationship between annual ET and growing season length simulated by the original and modified SWAT models revealed that the original SWAT model was unable to accurately describe the intermediate process variables of the hydrological cycle. Process-based hydrological models should be configured to consider the accuracy of plant growth dynamics simulation, which could reduce the number of calibration parameter and help avoid overparameterization for runoff simulation at the cost of other hydrological processes. The vegetation growth module and algorithms used to combine remote sensing data with the SWAT model can generalized to other watershed models and be applied to support water resources planning and management that require understanding of the coupled ecological and hydrological processes.

Acknowledgments

This study was supported by the National Science Fund for Distinguished Young Scholars (42025101), International Cooperation and Exchanges NSFC-STINT (42111530181), General Program of National Nature science foundation of China (No. 31770516), and the 111 Project (B18006). The authors gratefully acknowledge all members of the Hydrological Yearbook of the People's Republic of China for providing the in situ runoff data. We thank James Buxton from Liwen Bianji (Edanz) for editing the English text of this manuscript.

Open Research

Details of relevant meteorological driving data and measured verification data can be obtained from the data description section in this paper.

References

http://srtm

Abbaspour, K. C. (2008), SWAT calibration and uncertainty programs, *A User Manual. Eawag Zurich, Switzerland*, *20.*Abbaspour, K. C., C. Johnson, and M. T. Van Genuchten (2004), Estimating uncertain flow and transport parameters

using a sequential uncertainty fitting procedure, *Vadose zone journal*, *3*(4), 1340-1352.Abiodun, O. O., H. Guan, V. E. Post, and O. Batelaan (2018), Comparison of MODIS and SWAT evapotranspiration over a complex terrain at different spatial scales, *Hydrology and Earth System Sciences*, *22*(5), 2775-2794.Alemayehu, T., A. v. Griensven, B. T. Woldegiorgis, and W. Bauwens (2017), An improved SWAT vegetation growth module and its evaluation for four tropical ecosystems, *Hydrology and Earth System Sciences*, *21*(9), 4449-4467.Allen, R. G. (1986), A Penman for all seasons, *Journal of Irrigation and Drainage Engineering*, *112*(4), 348-368.Allen, R. G., M. E. Jensen, J. L. Wright, and R. D. Burman (1989), Operational estimates of reference evapotranspiration, *Agronomy journal*, *81*(4), 650-662.Arnold, J. G., R. Srinivasan, R. S. Muttiah, and J. R. Williams (1998), Large area hydrologic modeling and assessment part I: model development 1, *JAWRA Journal of the American Water Resources Association*, *34*(1), 73-89.Arnold, J. G., D. N. Moriasi, P. W. Gassman, K. C. Abbaspour, M. J. White, R. Srinivasan, C. Santhi, R. Harmel, A. Van Griensven, and M. W. Van Liew (2012), SWAT: Model use, calibration, and validation, *Transactions of the ASABE*, *55*(4), 1491-1508.Badeck, F.-W., A. Bondeau, K. Bottcher, D. Doktor, W. Lucht, J. Schaber, and S. Sitch (2004), Responses of spring phenology to climate change, *New Phytologist*, *162*(2), 295-309.Beven, K. (2002), Towards a coherent philosophy for environmental modelling, *Proceedings of the Royal Society A: Mathematical, Physical and Engineering Sciences*, *458*(2026), 2465-2484.Boswell, V. (1926), The influence of temperature upon the growth and yield of garden peas, paper presented at Proc. Amer. Soc. Hort. Sci.Chen, J., P. Jönsson, M. Tamura, Z. Gu, B. Matsushita, and L. Eklundh (2004), A simple method for reconstructing a high-quality NDVI time-series data set based on the Savitzky–Golay filter, *Remote Sensing of Environment*, *91*(3-4), 332-344.Chuine, I., and J. Régnière (2017), Process-based models of phenology for plants and animals, *Annual Review of Ecology, Evolution, and Systematics*, *48*, 159-182.Cong, N., S. Piao, A. Chen, X. Wang, X. Lin, S. Chen, S. Han, G. Zhou, and X. Zhang (2012), Spring vegetation green-up date in China inferred from SPOT NDVI data: A multiple model analysis, *Agricultural and Forest Meteorology*, *165*, 104-113.Delbart, N., G. Picard, T. Le Toan, L. Kergoat, S. Quegan, I. Woodward, D. Dye, and V. Fedotova (2008), Spring phenology in boreal Eurasia over a nearly century time scale, *Global Change Biology*, *14*(3), 603-614.Fan, D., X. Zhao, W. Zhu, W. Sun, and Y. Qiu (2020), An improved phenology model for monitoring green-up date variation in Leymus chinensis steppe in Inner Mongolia during 1962–2017, *Agricultural and Forest Meteorology*, *291*, 108091.Fu, Y., X. Li, X. Zhou, X. Geng, Y. Guo, and Y. Zhang (2020), Progress in plant phenology modeling under global climate change, *Science China Earth Sciences*, *63*(9), 1237-1247.Fu, Y. H., H. Zhao, S. Piao, M. Peaucelle, S. Peng, G. Zhou, P. Ciais, M. Huang, A. Menzel, and J. Peñuelas (2015), Declining global warming effects on the phenology of spring leaf unfolding, *Nature*, *526*(7571), 104-107.Geng, X., X. Zhou, G. Yin, F. Hao, X. Zhang, Z. Hao, V. P. Singh, and Y. H. Fu (2020), Extended growing season reduced river runoff in Luanhe River basin, *Journal of Hydrology*, *582*, 124538.Gill, A. L., A. S. Gallinat, R. Sanders-DeMott, A. J. Rigden, D. J. Short Gianotti, J. A. Mantooth, and P.

H. Templer (2015), Changes in autumn senescence in northern hemisphere deciduous trees: a meta-analysis of autumn phenology studies, *Annals of botany*, *116*(6), 875-888.Hargreaves, G. H., and Z. A. Samani (1985), Reference crop evapotranspiration from temperature, *Applied engineering in agriculture*, *1*(2), 96-99.Hufkens, K., D. Basler, T. Milliman, E. K. Melaas, and A. D. Richardson (2018), An integrated phenology modelling framework in R, *Methods in Ecology and Evolution*, *9*(5), 1276-1285.Jarvis, A., H. I. Reuter, A. Nelson, and E. Guevara (2008), Hole-filled SRTM for the globe Version 4, *available from the CGIAR-CSI SRTM 90m Database (. csi. cgiar. org)*, *15*, 25-54.Jeong, S. J., C. H. HO, H. J. GIM, and M. E. Brown (2011), Phenology shifts at start vs. end of growing season in temperate vegetation over the Northern Hemisphere for the period 1982–2008, *Global change biology*, *17*(7), 2385-2399.Jobling, M. (1997), Temperature and growth: modulation of growth rate via temperature change, paper presented at Seminar series-society for experimental biology, Cambridge University Press.Kergoat, L. (1998), A model for hydrological equilibrium of leaf area index on a global scale, *Journal of hydrology*, *212*, 268-286.Kim, N. W., I. M. Chung, Y. S. Won, and J. G. Arnold (2008), Development and application of the integrated SWAT–MODFLOW model, *Journal of hydrology*, *356*(1-2), 1-16.Kirchner, J. W. (2006), Getting the right answers for the right reasons: Linking measurements, analyses, and models to advance the science of hydrology, *Water Resources Research*, *42*(3).Liu, Q., Y. H. Fu, Z. Zhu, Y. Liu, Z. Liu, M. Huang, I. A. Janssens, and S. Piao (2016), Delayed autumn phenology in the Northern Hemisphere is related to change in both climate and spring phenology, *Global change biology*, *22*(11), 3702-3711.Ma, T., Z. Duan, R. Li, and X. Song (2019), Enhancing SWAT with remotely sensed LAI for improved modelling of ecohydrological process in subtropics, *Journal of Hydrology*, *570*, 802-815.Magoon, C. A., and C. W. Culpepper (1932), Response of sweet corn to varying temperatures from time of planting to canning maturity.Marini, F., and B. Walczak (2015), Particle swarm optimization (PSO). A tutorial, *Chemometrics and Intelligent Laboratory Systems*, *149*, 153-165.Monteith, J. L. (1965), Evaporation and environment, paper presented at Symposia of the society for experimental biology, Cambridge University Press (CUP) Cambridge.Moriasi, D. N., J. G. Arnold, M. W. Van Liew, R. L. Bingner, R. D. Harmel, and T. L. Veith (2007), Model evaluation guidelines for systematic quantification of accuracy in watershed simulations, *Transactions of the ASABE*, *50*(3), 885-900.Nachtergaele, F., H. van Velthuizen, L. Verelst, N. Batjes, K. Dijkshoorn, V. van Engelen, G. Fischer, A. Jones, and L. Montanarela (2010), The harmonized world soil database, paper presented at Proceedings of the 19th World Congress of Soil Science, Soil Solutions for a Changing World, Brisbane, Australia, 1-6 August 2010.Neitsch, S. L., J. G. Arnold, J. R. Kiniry, and J. R. Williams (2011), Soil and water assessment tool theoretical documentation version 2009, Texas Water Resources Institute.Parajuli, P. B., P. Jayakody, and Y. Ouyang (2018), Evaluation of using remote sensing evapotranspiration data in SWAT, *Water resources management*, *32*(3), 985-996.Peñuelas, J., and I. Filella (2009), Phenology feedbacks on climate change, *Science*, *324*(5929), 887-888.Piao, S., J. Fang, L. Zhou, P. Ciais, and B. Zhu (2006), Variations in satellite-derived phenology

in China's temperate vegetation, *Global change biology*, *12*(4), 672-685.Piao, S., G. Yin, J. Tan, L. Cheng, M. Huang, Y. Li, R. Liu, J. Mao, R. B. Myneni, and S. Peng (2015), Detection and attribution of vegetation greening trend in China over the last 30 years, *Global change biology*, *21*(4), 1601-1609.Piao, S., Q. Liu, A. Chen, I. A. Janssens, Y. Fu, J. Dai, L. Liu, X. Lian, M. Shen, and X. Zhu (2019), Plant phenology and global climate change: Current progresses and challenges, *Global change biology*, *25*(6), 1922-1940.Priestley, C. H. B., and R. J. TAYLOR (1972), On the assessment of surface heat flux and evaporation using large-scale parameters, *Monthly weather review*, *100*(2), 81-92.Rajib, A., I. L. Kim, H. E. Golden, C. R. Lane, S. V. Kumar, Z. Yu, and S. Jeyalakshmi (2020), Watershed modeling with remotely sensed big data: MODIS leaf area index improves hydrology and water quality predictions, *Remote Sensing*, *12*(13), 2148.Reed, B. C., J. F. Brown, D. VanderZee, T. R. Loveland, J. W. Merchant, and D. O. Ohlen (1994), Measuring phenological variability from satellite imagery, *Journal of vegetation science*, *5*(5), 703-714.Richardson, A. D., A. S. Bailey, E. G. Denny, C. W. Martin, and J. O'KEEFE (2006), Phenology of a northern hardwood forest canopy, *Global Change Biology*, *12*(7), 1174-1188.Richardson, A. D., T. F. Keenan, M. Migliavacca, Y. Ryu, O. Sonnentag, and M. Toomey (2013), Climate change, phenology, and phenological control of vegetation feedbacks to the climate system, *Agricultural and Forest Meteorology*, *169*, 156-173.Richardson, A. D., R. S. Anderson, M. A. Arain, A. G. Barr, G. Bohrer, G. Chen, J. M. Chen, P. Ciais, K. J. Davis, and A. R. Desai (2012), Terrestrial biosphere models need better representation of vegetation phenology: results from the N orth A merican C arbon P rogram S ite S ynthesis, *Global Change Biology*, *18*(2), 566-584.Rodriguez-Iturbe, I. (2000), Ecohydrology: A hydrologic perspective of climate-soil-vegetation dynamies, *Water Resources Research*, *36*(1), 3-9.Rohde, A., and R. P. Bhalerao (2007), Plant dormancy in the perennial context, *Trends in plant science*, *12*(5), 217-223.Ruddell, B. L., D. T. Drewry, and G. S. Nearing (2019), Information theory for model diagnostics: Structural error is indicated by trade-off between functional and predictive performance, *Water Resources Research*, *55*(8), 6534-6554.Savitzky, A., and M. J. Golay (1964), Smoothing and differentiation of data by simplified least squares procedures, *Analytical chemistry*, *36*(8), 1627-1639.Shukla, P., J. Skea, E. Calvo Buendia, V. Masson-Delmotte, H. Pörtner, D. Roberts, P. Zhai, R. Slade, S. Connors, and R. Van Diemen (2019), IPCC, 2019: Climate Change and Land: an IPCC special report on climate change, desertification, land degradation, sustainable land management, food security, and greenhouse gas fluxes in terrestrial ecosystems.Sprenger, M., H. Leistert, K. Gimbel, and M. Weiler (2016), Illuminating hydrological processes at the soil-vegetation-atmosphere interface with water stable isotopes, *Reviews of Geophysics*, *54*(3), 674-704.Stein, M. (1987), Large sample properties of simulations using Latin hypercube sampling, *Technometrics*, *29*(2), 143-151.Strauch, M., and M. Volk (2013), SWAT plant growth modification for improved modeling of perennial vegetation in the tropics, *Ecological Modelling*, *269*, 98-112.Tesemma, Z., Y. Wei, M. Peel, and A. Western (2015), The effect of year-to-year variability of leaf area index on Variable Infiltration Capacity model performance and simulation of runoff, *Ad-*

vances in Water Resources, *83*, 310-322.Valencia, S., J. F. Salazar, J. C. Villegas, N. Hoyos, and M. Duque-Villegas (2021), SWAT-Tb with improved LAI representation in the tropics highlights the role of forests in watershed regulation, *Earth and Space Science Open Archive ESSOAr*.Villamizar, S. R., S. M. Pineda, and G. A. Carrillo (2019), The effects of land use and climate change on the water yield of a watershed in Colombia, *Water*, *11*(2), 285.Wagner, P., S. Kumar, P. Fiener, and K. Schneider (2011), Hydrological modeling with SWAT in a monsoon-driven environment: experience from the Western Ghats, India, *Transactions of the ASABE*, *54*(5), 1783-1790.Wang, H., C. Wu, P. Ciais, J. Penuelas, J. Dai, Y. Fu, and Q. Ge (2020), Overestimation of the effect of climatic warming on spring phenology due to misrepresentation of chilling, *Nature communications*, *11*(1), 1-9.Webb, A. A., and A. Kathuria (2012), Response of streamflow to afforestation and thinning at Red Hill, Murray Darling Basin, Australia, *Journal of Hydrology*, *412*, 133-140.Wei, X., and M. Zhang (2010), Quantifying streamflow change caused by forest disturbance at a large spatial scale: A single watershed study, *Water resources research*, *46*(12).White, M. A., P. E. Thornton, and S. W. Running (1997), A continental phenology model for monitoring vegetation responses to interannual climatic variability, *Global biogeochemical cycles*, *11*(2), 217-234.White, M. A., K. M. de Beurs, K. Didan, D. W. Inouye, A. D. Richardson, O. P. Jensen, J. O'keefe, G. Zhang, R. R. Nemani, and W. J. van Leeuwen (2009), Intercomparison, interpretation, and assessment of spring phenology in North America estimated from remote sensing for 1982–2006, *Global Change Biology*, *15*(10), 2335-2359.Williams, J., C. Jones, J. Kiniry, and D. A. Spanel (1989), The EPIC crop growth model, *Transactions of the ASAE*, *32*(2), 497-0511.Xiao, Z., S. Liang, J. Wang, P. Chen, X. Yin, L. Zhang, and J. Song (2013), Use of general regression neural networks for generating the GLASS leaf area index product from time-series MODIS surface reflectance, *IEEE Transactions on Geoscience and Remote Sensing*, *52*(1), 209-223.Yang, Q., and X. Zhang (2016), Improving SWAT for simulating water and carbon fluxes of forest ecosystems, *Science of the Total Environment*, *569*, 1478-1488.Yang, Q., X. Zhang, J. E. Almendinger, M. Huang, G. Leng, Y. Zhou, K. Zhao, G. R. Asrar, X. Li, and J. Qiu (2019), Improving the SWAT forest module for enhancing water resource projections: A case study in the St. Croix River basin, *Hydrological Processes*, *33*(5), 864-875.Yu, H., E. Luedeling, and J. Xu (2010), Winter and spring warming result in delayed spring phenology on the Tibetan Plateau, *Proceedings of the National Academy of Sciences*, *107*(51), 22151-22156.Yuan, M., L. Zhao, A. Lin, Q. Li, D. She, and S. Qu (2020), How do climatic and non-climatic factors contribute to the dynamics of vegetation autumn phenology in the Yellow River Basin, China?, *Ecological Indicators*, *112*.Zhang, D., X. Liu, and P. Bai (2018), Different influences of vegetation greening on regional water-energy balance under different climatic conditions, *Forests*, *9*(7), 412.Zhang, H., B. Wang, D. Li Liu, M. Zhang, L. M. Leslie, and Q. Yu (2020), Using an improved SWAT model to simulate hydrological responses to land use change: A case study of a catchment in tropical Australia, *Journal of Hydrology*, *585*, 124822.Zhu, Z., et al. (2016), Greening of the Earth and its drivers, *Nature Climate Change*, *6*(8), 791-795.